Experimental behaviour of extended end-plate composite beam-to-column joints subjected to reversal of loading

Xiamin Hu[†], Desheng Zheng[‡] and Li Yang[‡]

College of Civil Engineering, Nanjing University of Technology, 210009, Nanjing, China

Abstract. This paper is concerned with the behaviour of steel and concrete composite joints subjected to reversal of loading. Three cruciform composite joint specimens and one bare steel joint specimen were tested so that one side of the beam-to-column connection was under negative moment and another side under positive moment. The steelwork beam-to-column connections were made of bolted end plate with an extended haunch section. Composite slabs employing metal decking were used for all the composite joint specimens. The moment-rotation relationships for the joints were obtained experimentally. Details of the experimental observations and results were reported.

Keywords: composite joints; cyclic loading; moment rotational response.

1. Introduction

Steel moment-resisting frames with welded beam-to-column connections were damaged during the 1994 Northridge earthquake and the 1995 Hyogoken-Nanbu earthquake. These earthquakes arouse engineers to resurvey the behavior of connections. The semi-rigid connection has received widely attention because of its good seismic performance and significant economic efficiency. Extensive work has been carried out during the past decade on the steel and concrete composite joints leading to acceptance of semi-rigid design of building frames. Some experiments indicate that concrete slab above steel beam has great importance on moment resistance, initial stiffness and rotation capacity of composite joints (Altmann *et al.* 1991, Davison *et al.* 1990, Leon 1990, da Silva 2001, Li *et al.* 1996, Hu *et al.* 2002, 2004, Xiao *et al.* 1994). Experimental research on the behaviour of composite joints under cyclic loading can be traced back to tests performed by Ammerman and Leon (1987). Over the past several years, many researches has been conducted on the cyclic behaviuor of composite joints (Liu and Astaneh-Asl 1989, Lee and Lu 1989, Sheikh *et al.* 1989, Benussi and Zandonini 1991, Plumier and Schleich 1993, Pradohan and Bouwkamp 1994, Leon *et al.* 1998, Liew *et al.* 2004).

The work presented herein provides an experimental study on the hysteretic behavior of extended end-plate composite joints subjected to reversal of loading. This research will explore its applicability to the steel and concrete composite residential building system. One bare steel joint

† Professor, Corresponding author, E-mail: verbundbau@163.com
‡ Graduate Student

specimen and three composite partially extended end-plate specimens were tested under reversal of loads. Effects of composite slabs and reinforcement ratio on hysteretic behavior of joints were considered during cyclic loading. Results of the experiment show that partially extended end-plate composite joints have good seismic performances, and the longitudinal reinforcement ratio has significant influence on connection behaviours. Details of the experimental observations and results were reported.

2. Experimental investigation

2.1 Specimens and test setup

Three composite cruciform joint specimens and one bare cruciform joint specimen denoted as J17 to J20, respectively, were tested to failure. This is to simulate the internal beam-to-column joints in a composite frame. All four specimens were designed with exactly the same steel details. The three
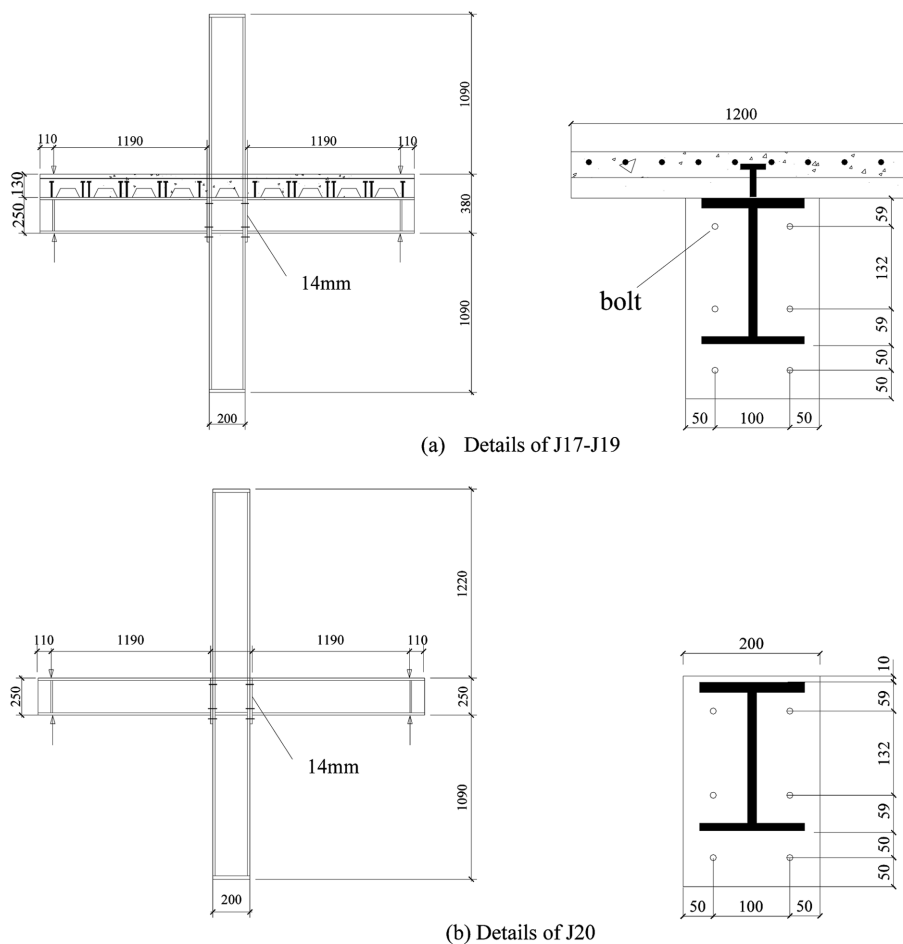

(a) Details of J17-J19

(b) Details of J20

Fig. 1 Details of specimens

composite specimens J17, J18 and J19 and the one bare steel specimens J20 were the cruciform arrangement as shown in Fig. 1. Here a smaller depth of steel beam was chosen to meet the demand for the lower cost and the more useable clear space in the steel and concrete composite residential building system. Two rolled steel beams HN250 × 125 of 1300 mm long were connected to a column HW200 × 200 by means of 14 mm thick extended end plate and M20 Grade 8.8 bolts. The welds of beam flanges to the end plate are of full penetration groove welds, and the beam web is welded with fillet welds. The columns of these specimens were stiffened with transverse stiffeners to the web at the level of the bottom beam flange and at the level of the top beam flange.

Composite slabs employing metal decking were used for all the composite joint specimens; the metal decking was LYSAGHT 2W with the effective depth equal to 51 mm. The over depth of concrete slab was 130 mm, with a width 1200 mm. Headed studs of 19 mm diameter and total post-welded height 100 mm were adopted as shear connectors. To achieve full interaction between the steel beam and concrete slab, two shear connectors were welded in each through of the metal decking.

The longitudinal reinforcement ratio for specimens J17, J18 and J19 is 0.95%, 1.48% and 1.91%, respectively. Longitudinal reinforcements of diameter 12 mm or 16 mm were distributed in one layer with equal spacing over the width of the slab.

All the material properties of steel are summarized in Table 1 and the concrete cube test results are given in Table 2.

A typical test setup was used to investigate the behaviour of composite joints subjected to reversal of loading (Yang 2004). The over specimen geometry and loading configuration are shown in Fig. 2. A axial load of 400 kN was applied to simulate the dead load that an actual column would experience. The history of loading procedure is illustrated in Fig. 3, where P is the applied load on the end of beam; P_y is yield load of the connection; Δ is the displacement of beam; Δ_y is the yield displacement of beam. Before the reinforcements in the slab yield, loading increment based on force control was used. Subsequently, displacement control was applied. The successive loading at $1.0\Delta_y$,

Table 1 Material properties of steel

Component		Yield strength $f_y/\text{N·mm}^{-2}$	Ultimate strength $f_u/\text{N·mm}^{-2}$	Young's modulus $E_s/\text{N·mm}^{-2}$
Rebar	$\varphi12$	229	376	1.91×10^5
	$\varphi16$	273.6	417.9	2.25×10^5
Stud	$\varphi19\times100$	387	484	—
Bolt	8.8 M20	830	—	2.73×10^5
End-plate	14 mm	245.5	479.9	1.6×10^5
Stiffening	9 mm	230	547.9	1.62×10^5

Table 2 Mechanical properties of concrete

Specimens	Age/d	Type of specimen	Comp. strength $f_{cu}/\text{N·mm}^{-2}$	Young's modulus $E_c/\text{N·mm}^{-2}$
J17	50	150 mm cube	35.6	3.16×10^4
J18	50	150 mm cube	32.9	3.09×10^4
J19	50	150 mm cube	32.9	3.09×10^4
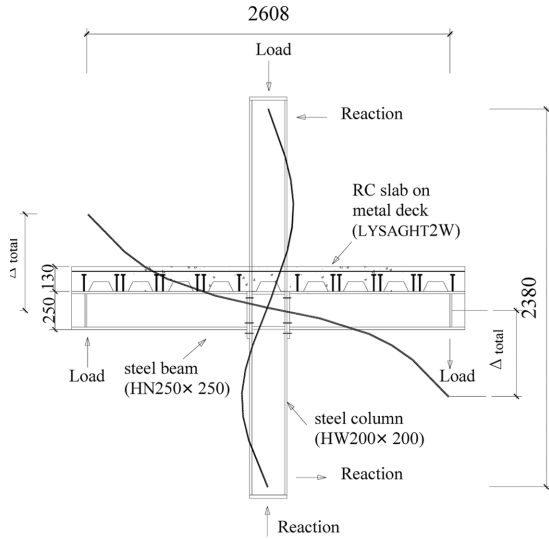
Fig. 2 Test setup
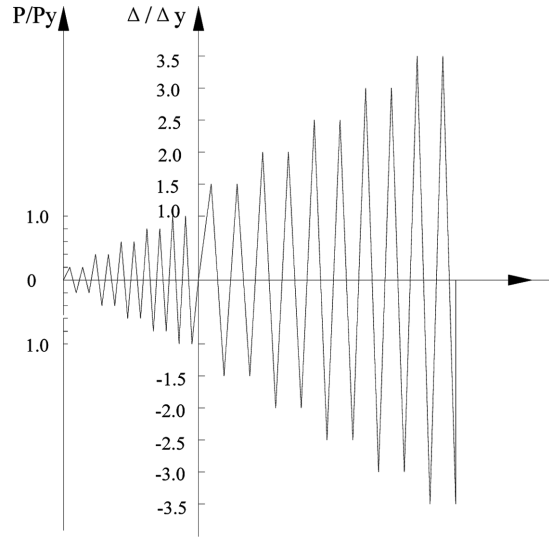
Fig. 3 Typical loading procedure for cyclic test

(a) Arrangement of strain gauges
on reinforcement

(b) Gauges arrangement on
panel zone and beam web

(c) Gauges arrangement
on beam flanges

(d) Gauges arrangement
on traverse stiffener

(e) Gauges arrangement
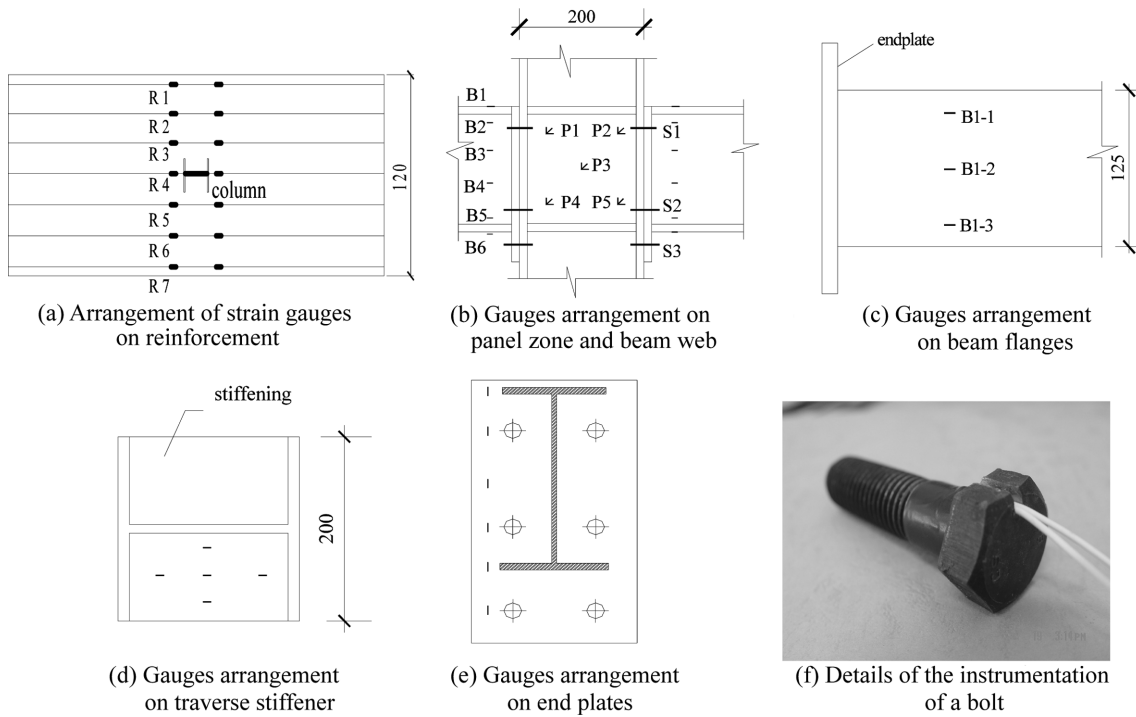on end plates

(f) Details of the instrumentation
of a bolt

Fig. 4 Gauges arrangement on crucial locations

$1.5\Delta_y$, $2.0\Delta_y$, $2.5\Delta_y$ and thereafter were performed. Force control for the loading and unloading branches and Displacement control for the loading and reloading branches were used alternately. A test was terminated when the specimen was failure.
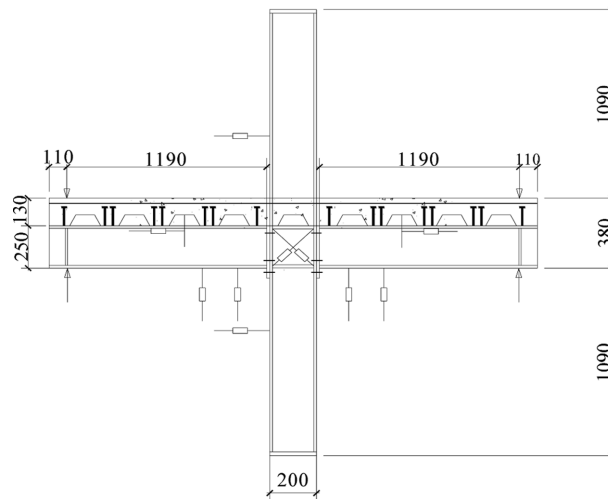
Fig. 5 Arrangement of transducers

2.2 Instrumentation

The main object of the test was to research the response of the composite joint subjected to the reversal of loading in terms of moment-rotation ($M - \varphi$) relationships. Moment was calculated using the equilibrium of the force. Rotation was measured by using inclinometers and counter checked with readings from the displacement transducers. Strains in the reinforcement and on the steel beam were measured using strain gauges (Fig. 4(a), Fig. 4(b), Fig. 4(c), Fig. 4(d) and Fig. 4(e)). Strain gauges were placed on some bolts to determine the tensile forces in the bolts at each of the load steps (Fig. 4(f)). Displacement transducers were used to measure the defection of the specimen on the beam bottom flange and the diagonal deflection in the panel zone (Fig. 5). These transducers were positioned close to the column flange to exclude the rotation due to bending of beam. In addition, two transducers were used measure the slip between the composite slab and steel beam (Fig. 5).

3. The test results

Detailed discussion of the test results is presented in the following sections. In all the curves shown in the discussion, positive and negative values represent positive and negative strains or positive and negative moments.

3.1 Specimen J20

J20 is a bare steel specimen used as a benchmark for comparison with other composite joint specimens. For the composite joint, extending the end plate towards the composite slab will not be useful for moment resistance since the rebars in composite slab are expected to provide major tensile resistance on negative moment. In order to comparison the composite joint specimens, Specimen J20 is also designed as an extended end plate steel joint, where the end plate was extended beyond the beam bottom flange.
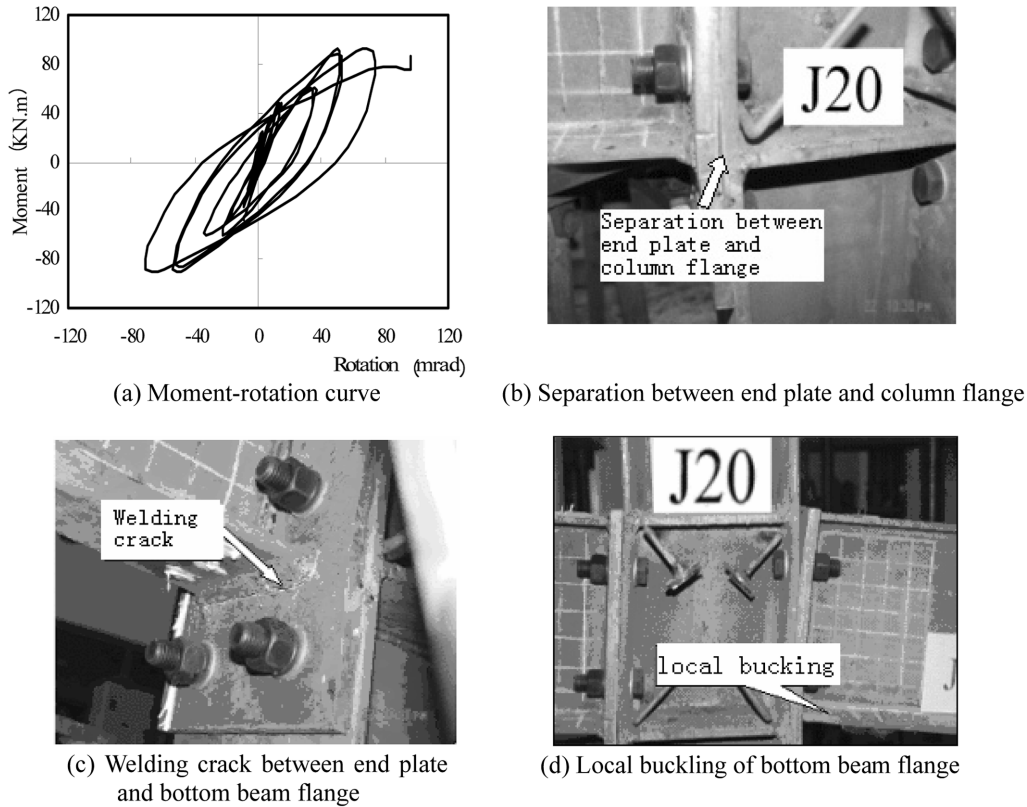
(a) Moment-rotation curve

(b) Separation between end plate and column flange

(c) Welding crack between end plate
and bottom beam flange

(d) Local buckling of bottom beam flange

Fig. 6 Test results of specimen J20

Connection moment versus connection rotation ($M - \varphi$) curve of specimen J20 is shown in Fig. 6(a). It can be observed in the test that the web of the column in the panel zone started to yield when the positive connection moment reached a value of 48 kN·m. The end plate and the lower stiffener in the panel zone started to yield and the end plate was separated from column flange when the positive moment increased beyond a value of 60 kN·m (Fig. 6(b)). The separation between end plate and column flange was in evidence at the first step of displacement control processes. Yielding of the upper stiffener in the panel zone was found when the connection moment was about 85 kN·m. At the final state, it was found that the panel zone was deformed excessively and the weld seam between the end plate and the bottom beam flange was torn (Fig. 6(c)). The slightly local buckling of the bottom flange of steel beams was observed (Fig. 6(d)).

3.2 Specimens J17, J18 and J19

J17, J18 and J19 were partially extended end plate joints with two shear studs per through though of metal decking, as shown in Fig. 1(a). They were designed to investigate effects of longitudinal reinforcement ratio on the behaviour of composite joints under the reversal of loading. Specimens J17, J18 and J19 had the same details except the reinforcement ratio of 0.95%, 1.48% and 1.91%, respectively. Connection moment versus connection rotation ($M - \varphi$) curves of J17, J19 is shown in
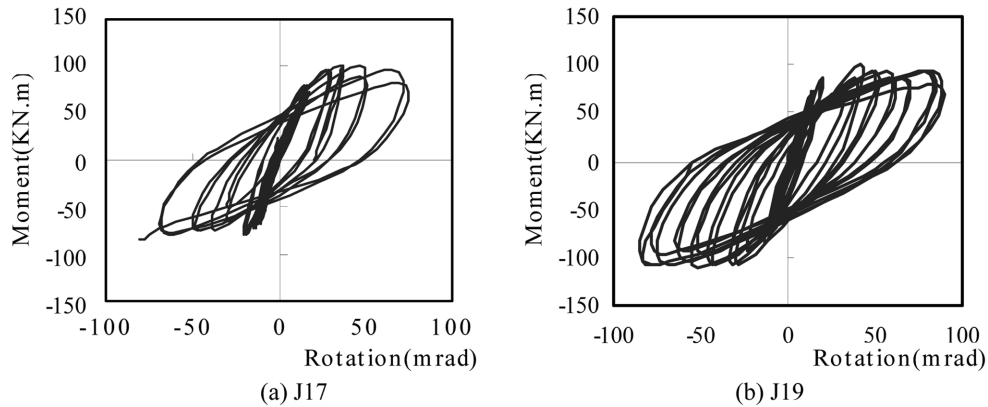
(a) J17   (b) J19

Fig. 7 Moment-rotation curves

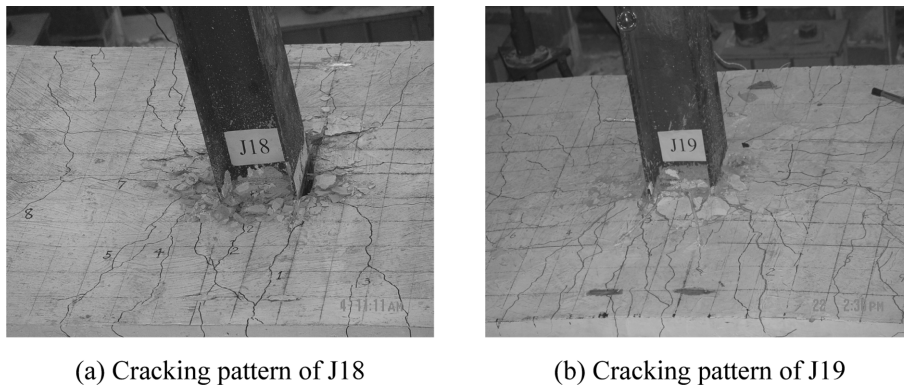(a) Cracking pattern of J18   (b) Cracking pattern of J19

Fig. 8 Cracking pattern of concrete slab

Fig. 7. The deformation of J18 could not be completely measured at the second step of displacement control processes due to faulty device.

The first crack of J17 was observed on the right slab when the hogging moment reached the values of 48 kN·m. The crack closed completely when force was unloaded to zero. The reversed loading was then applied. The cracking moment resistance for the left connection was also 48 kN·m. The crack started from the tip of column flange extended towards the edge with the increasing in the loads. The crack moments of J18 and J19 were all 36 kN·m. These values were slightly smaller than those of J17. This result shows that the cracking resistance of the composite joints is mainly controlled by the concrete strength. However, the slab reinforcement ratio had significantly effect on the cracking pattern. Compared to the crack pattern of J17, J18 and J19, it was found that the increase of the amount of the reinforcement resulted in finer crack and closer spacing. Comparison of the crack pattern of J18 and J19 is shown in Fig. 8.

The debonding of the concrete from the metal decking in specimen J17 was visible when the moment reached a value of 73 kN·m (Fig. 9(a)). Similarly, the same phenomenon also occurs in specimens J18 and J19 (Fig. 9(b)) respectively when the connection moment was 80 kN·m and 100 kN·m. The separation near panel zone was much serious than in other position because of larger shear deformation near the panel zone.
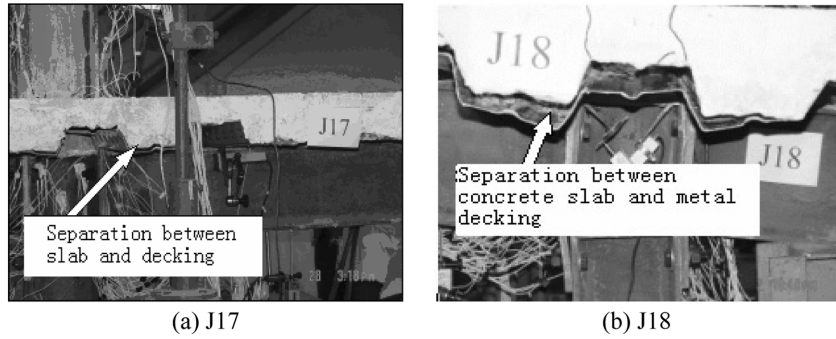
(a) J17   (b) J18

Fig. 9 Separation between concrete and metal decking

(a) Separation between end plate and   (b) Rupture of end plate of J17 beam
column flange of J17

(c)Welding failure of J17   (d) Separation between end plate and
column flange of J18

(e) Rupture of end plate of J18   (f) Welding failure of J19
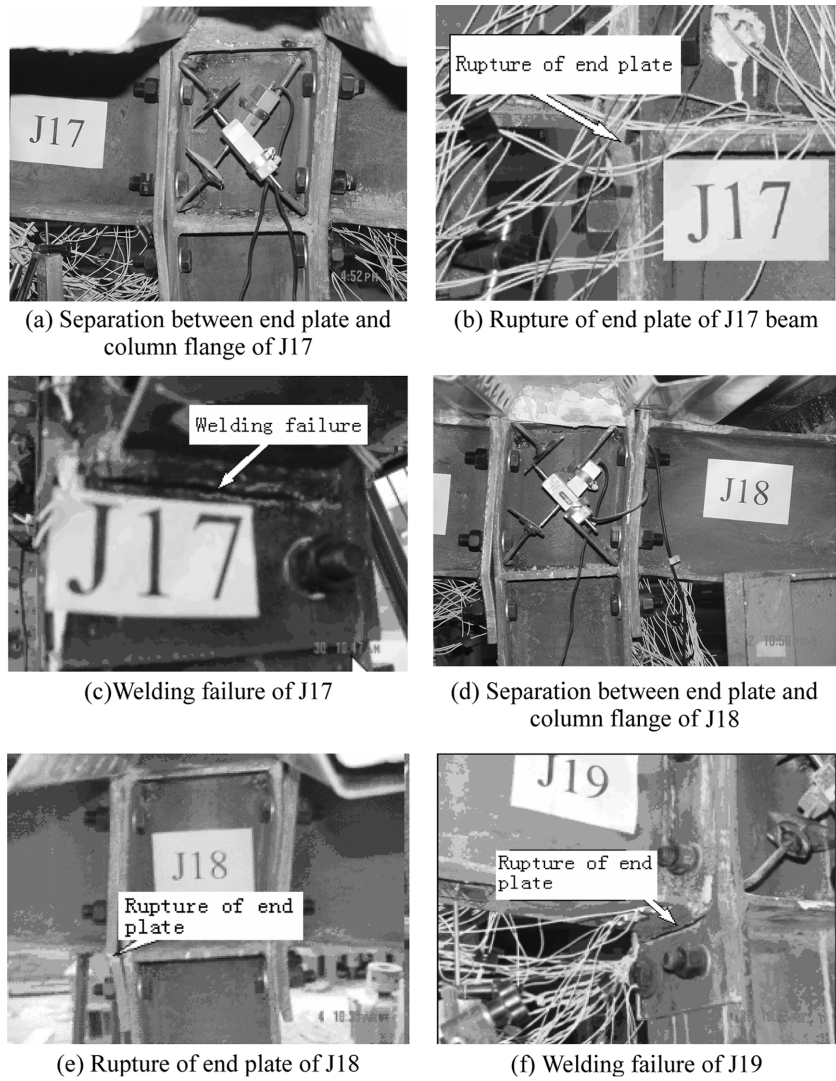
Fig. 10 Test results of end plate in specimen J17, J18 and J19
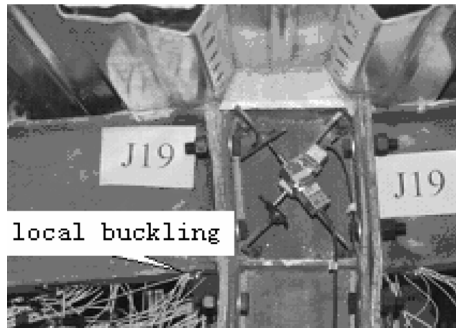
Fig. 11 Local buckling of beam bottom flange

Fig. 12 Crush of concrete around column

The separation between end plate and column flange in J17 was in evidence at the first step of displacement control processes, as shown in Fig. 10(a). As the increase of the load, the deformation of the end plate in J17 gradually increased until rupture suddenly at the limit (Fig. 10(b)). The low cyclic fatigue and the prying force resulted in the rupture of the extended end plate. At the final stage, it was observed that the weld seam between the end plate and the bottom beam flange was torn (Fig. 10(c)) and the panel zone was deformed excessively. The similar failure processes were also observed in J18 and J19 (Fig. 10).

At limit state, the slight local buckling of the bottom flange of steel beams was observed in J17 and J18, but the evident local buckling was found in J19 (Fig. 11). The final stage of the composite slab vicinity to the column is shown in Fig. 12. It is noted that the slab around the steel column is badly damaged.

4. Discussion of test results

4.1 Moment-rotation behaviour

The response of joint subjected to cyclic loading can be used to check the structural reliability. A joint can be considered as stable when the loss of strength and stiffness at large inelastic deformation due to cyclic loading is negligible. Connection moment versus connection rotation $(M - \varphi)$ curves of J17, J19 in Fig. 7 show that the loss of strength and stiffness is not significant when the rotation is smaller than 46 mrad. It was found that the strength and stiffness in second cycles are not less than 89% of that of first cycle.

The steel joint and the composite joints exhibit different moment-rotation responses under a reversal of loads. The maximum moments of J17, J18, J19 and J20 were 99.6, 109.4, 111.8 and 89.4 kN·m, and the corresponding initial stiffness values under negative moment were 21.7, 24.9, 28.1 and 7.26 kN·m/mrad, respectively. Comparison between composite joint and bare steel joint illustrates clearly the enhancement in moment capacity and stiffness due to composite action. The enhancement in moment capacity is primarily due to the tension resistance from the slab reinforcement. The moment capacity and initial stiffness increased with increasing of the reinforcement ratio. It should be noted that the moment capacity in J19 did not realize the value expected. This can be explained by the failure modes for the specimens. It is observed that the local buckling in J19 was more evidently than that in J17 and J18. This prevented specimen J19 from

Table 3 Characteristic rotation

Specimen	Under negative moment		Under positive moment	
	Yield rotation ϕ_y^- / mrad	Ultimate rotation ϕ_u^- / mrad	Yield rotation ϕ_y^+ / mrad	Ultimate rotation ϕ_u^+ / mrad
J17	11.3	69.2	16.6	68.8
J19	18.2	82.9	16.4	81.0
J20	8.1	66.7	13.8	66.1

attaining higher moment capacity. Therefore, the reinforcement ratio must be carefully selected to commensurate with the steel beam compression resistance.

The initial stiffness under positive moment was 5.48, 6.09, 6.16 and 3.92 kN·m/mrad for J17, J18, J19 and J20, respectively. Compared with the bare steel joint, the initial stiffness of the composite joint was evidently enhanced due to the action of the composite slab. However, the increase of the reinforcement ratio had no significant effect on the initial stiffness of composite joints under positive moment.

The yield rotations and ultimate rotations for J17, J19 and J20 were shown in Table 3 (The deformation of J18 could not be completely measured due to faulty device). The rotation capacity corresponding to the maximum moment in all the specimens was greater than 30 mrad. The moment-rotation curves in Fig. 7 show that the composite joints have the good rotation capacity, ductility and energy dissipation. Compared with the specimen J17, J19 and J20, it can be found composite joints achieved greater plastic rotations and energy dissipation capacity than similar bare steel joints.

4.2 Strain profile in the slab reinforcement

In the composite joints J17, J18 and J19, strain gauges were attached to measure the strain profile of longitudinal reinforcement across the width of concrete slab at a distance of 75 mm from the column flange and verify the contribution of longitudinal reinforcement on the moment resistance. The strain readings of specimen J17 under positive moment are plotted reference to its locations to form the strain profile, as shown in Fig. 13 (under positive moment). It is observed that the
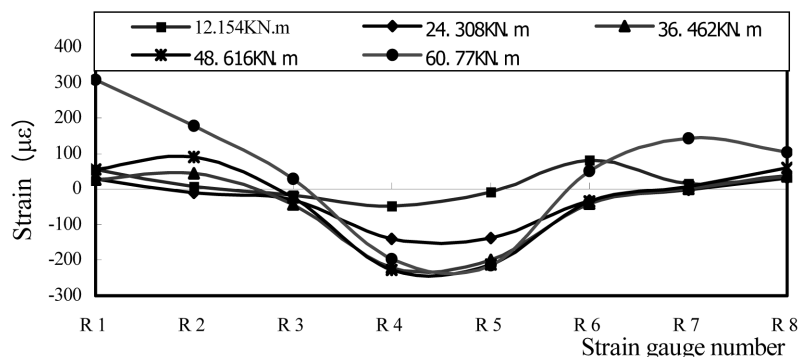

Fig. 13 Strain distribution on slab reinforcements in J17 under positive moment
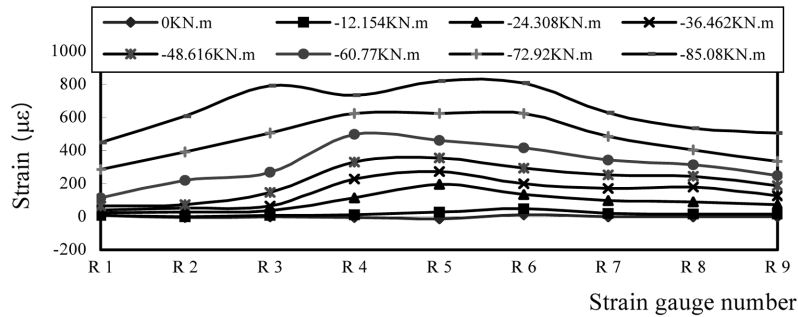
Fig. 14 Strain distribution on slab reinforcements in J19 under negative moment

compressive strain was recorded near the center of the slab and the compressive strain value turned gradually into the tensile strain value towards the slab edge. Therefore, when the composite joint is subjected to positive bending, the concrete slab is pushed against the column flange and the effective bearing width should be taken as the column flange width. It can be assumed that the stress distribution is uniform.

The strain profile on the slab reinforcements in J19 under the negative moment was plotted as shown in Fig. 14. It observed that the highest tensile stress was located near the center of the slab and the strain value decreased towards the slab edge. This variation in the slab reinforcement occurs because of shear lag. The strain profile gradually inclined to uniform across the width of the concrete slab with increasing of the applied load.

4.3 Strain profile in the steel beam section

In all the specimens, strain gauges were attached to measure the strain profile across the steel beam section, as shown in Fig. 4. The strain gauges are assumed to be located at the beam-column connection because they were attached close enough to the column flange. Strain profiles of J17 (under positive moment) and J19 (under negative moment) were plotted as shown in Fig. 15(a)
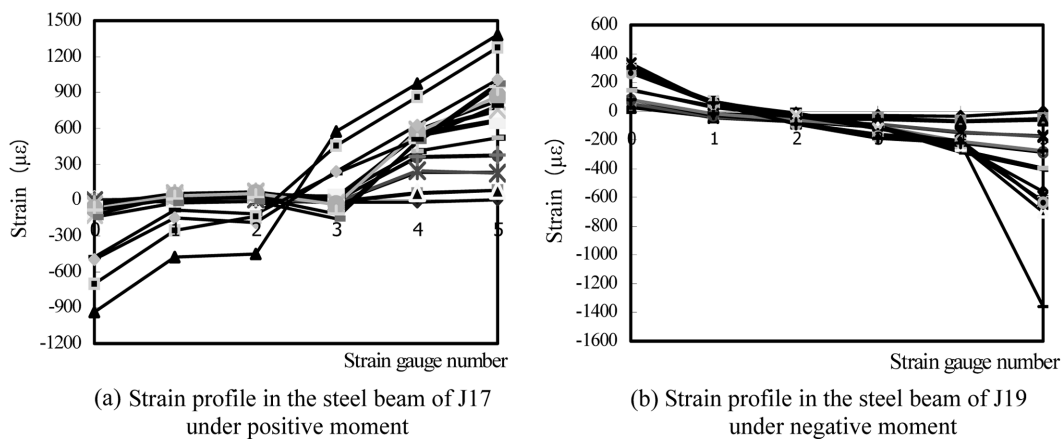
(a) Strain profile in the steel beam of J17 under positive moment

(b) Strain profile in the steel beam of J19 under negative moment

Fig. 15 Strain profile in steel beam under increasing moment

(a) Bolt strain under negative moment   (b) Bolt strain under positive moment
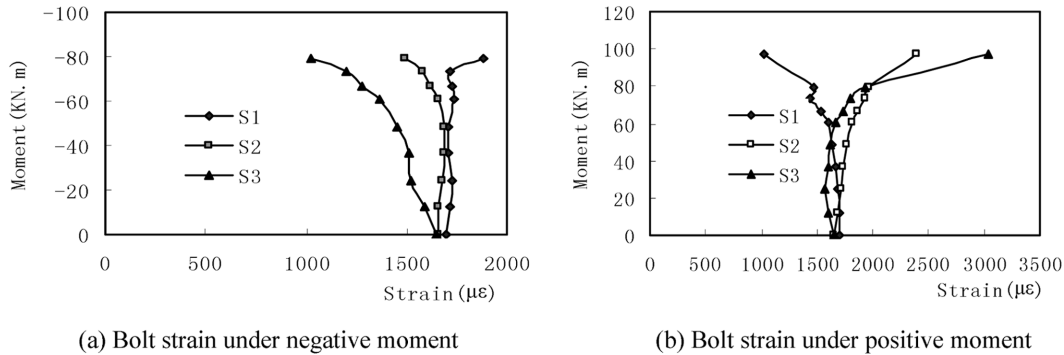
Fig. 16 Moment vs bolt strain of J17

and Fig. 15(b), respectively. For the composite beams, the location of neutral axis is mostly located at the beam web of the steel beam under negative moment and it shifts to the concrete slab under positive moment. However, it was found that the location of neutral axis in the composite joint was at the beam web both under positive moment and negative moment. It is evident that the smaller effective width in composite joints under positive moment resulted in increase of neutral axis depth.

4.4 Bolt response

M20 grade 8.8 bolts were tightened using a torque spanner to 370 N·m to ensure consistency. This torque level is equivalent to prestressing the bolts to an average force of 140 kN. The variations of the bolt strain with connection moment in J17 are plotted in Fig. 16(a) and Fig. 16(b). It was found that the pretension forces in the bolt remained constant at the lower loading cycles. As the cycles increased, the bottom bolt forces gradually decrease as compression force was applied to the column flange under negative moment. When joint was subjected to positive moment, strain of the bottom bolts quickly increased at the final stage. This observation shows that the neutral axis of J17 was located in the steel web.

4.5 Column web stiffener response

The variations of the column web stiffener strain with connection moment in J19 are plotted in Fig. 17(a) and Fig. 17(b).

Under a positive moment, the stiffener on the upper side was in compression and the stiffener on the lower side was in tension. The strain was small due to the effect of prestressing in the bolts at the lower loading cycles. As the cycles were increased, the stiffener strain gradually increased. The rupture of the extended end plate resulted in sudden reducing of the stiffener strain, when positive moment reached 99.9 kN·m value (Fig. 17(a)). When the strain was reduced to a certain value, it began to increase again, because the ruptured extend end plate acted as the flush end plate at this moment.

Under a negative moment, the stiffener on the upper side was in tension and the stiffener on the lower side was in compression. The strains of column web stiffeners were very small until the
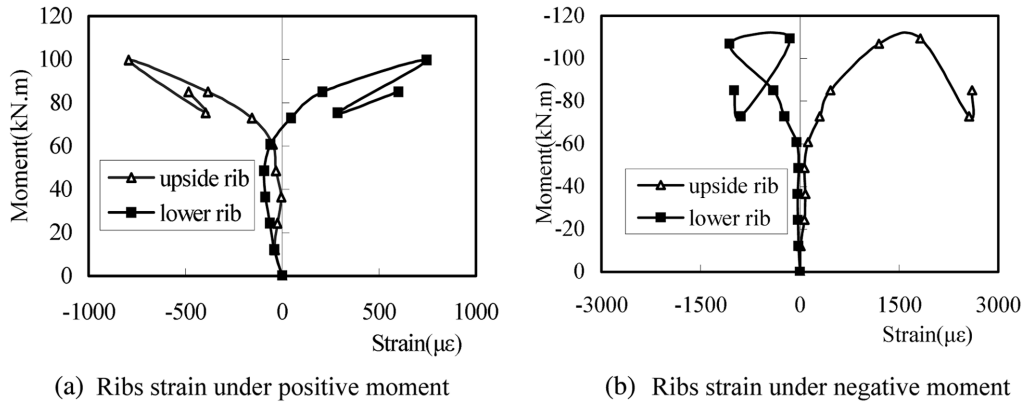
(a) Ribs strain under positive moment (b) Ribs strain under negative moment

Fig. 17 Moment vs column web strain of J19

moment reached −61 kN·m, which was due to the effect of prestressing in the bolts. With the increase of the load, the strain of the stiffener gradually increased until the moment reached the maximum value. It was observed that the stiffener strains under negative moment were greater than that under positive moment and had reached the yielding value.

The effects of column web stiffener are more significant under negative moment than under positive moment. In order to prevent the column web buckling, the column web stiffener should be used to design a composite connection.

4.6 Panel zone response

Column web panel shear distortion recorded by the diagonal transducer for J17 and J19 are shown in Fig. 18. No significant drop in resistance or stiffness was observed until the final stage in test. This result showed that the panel zone of composite joints is very ductile as in steel joint. However, the effective depth of panel zone in composite joint is higher than that of bare steel joint since the composite slab will increase the moment level arm. Thus, higher panel zone depth will lead to smaller panel shear force under the same moment and less shear deformation in panel zone is expected for composite joint than for steel joint.
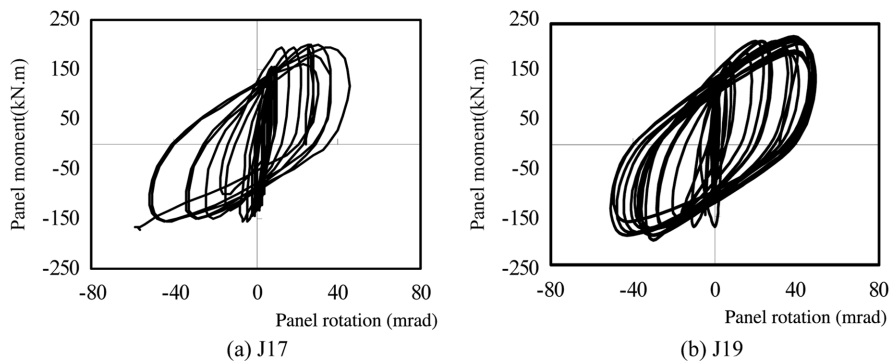

(a) J17 (b) J19

Fig. 18 Panel moment-panel rotation curves

4.7 Weld seam response

It was observed that the weld seam between the end plate and the bottom beam flange was torn for all specimens in the cycles of the test. As the increase of cycle number, the weld failed due to low cycle fatigue. The groove weld of bottom beam flange for the bare steel joint failed at the first cycle of amplitude $2.5\Delta_y$, while the same welds for the composite specimens failed at the first or second cycle of amplitude $3.5\Delta_y \sim 5\Delta_y$. With the addition of a composite floor slab the connection behaviour was improved.

5. Conclusions

Four extended end plate joint specimens (three composite joints with the composite metal deck floor and one bare steel joint) were tested and their details of the experimental behaviour under the reversal of loading was reported. The following conclusions can be drawn from the experimental research:

(1) The extended end plate joint with the composite metal deck floor has the good rotation and energy dissipating characteristics. It can be designed to be suitable for use in seismic force resisting moment frames of residential building system.

(2) The effects of the composite slab should be considered, since compared with the bare steel joint, the composite joint provides greater resistance and higher initial stiffness because of the composite action. The resistance in the composite joint subjected to negative moment increases with increasing of the slab reinforcement ratio, but this tendency exists up to a certain limiting value.

(3) The extended end plate has the good energy dissipating characteristics. However, the thickness of the end plate must be carefully selected to get the expected resistance.

(4) The panel zone of composite joints is very ductile as in steel joint. Higher panel zone depth will lead to smaller panel shear force under the same moment and less shear deformation in panel zone is expected for composite joint than those for steel joint.

(5) When the connection is subjected to positive moment, the effective compression width of the concrete slab should be taken as the column flange width.

Acknowlededgments

References

Altmann, R., Maquoi, R. and Jaspart, J.P. (1991), "Experimental study of the nonlinear behaviour of beam to column connections", *J. Const. Steel Res.*, **18**(1), 45-54.

Davison, J.B., Lam, D. and Nethercot, D.A. (1990), "Semi-rigid action of composite joints", *Struct. Eng.*, **68**(24), 18-22.

Hu, Xiamin, Guo, Yiqing, and Liu, Jianpin (2002), "Calculation of moment resistance of semi-rigid steel-concrete composite joints", *J. Nanjing Univ. Tech.*, **24**, 25-29.

Hu, Xiamin, Guo, Yiqing, and Liu, Jianpin (2004), "Initial roataion stiffness calculation of semi-rigid composite joints", *Industral Construction*, **34**, 71-73.

Lee, S.J. and Lu, L.W. (1989), "Cyclic tests of full-scale composite joints subassemblages", *J. Struct. Eng.*, **115**(8), 1977-1998.

Leon, R.T., Ammerman, D.J., Lin, J. and MeCauley, R.D. (1987), *Engng. J/Am Inst. Steel Construct*, 4th Quarter: 147-155.

Leon, R.T. (1990), "Semi-rigid composite construction", *J. Const. Steel Res.*, **15**, 99-120.

Leon, R.T., Hajjar, J.F. and Gustafson, M.A. (1998), "Seismic response of composite moment-resisting connections", I: Performance. *J. Struct. Eng.*, **124**(8), 868-876.

Leon, R.T., Hajjar, J.F. and Gustafson, M.A. (1998), "Seismic response of composite moment-resisting connections", II: Behaviour. *J. Struct. Eng.*, **124**(8), 877-885.

Li, T.Q., Moore, D.B., Nethercot, D.A. and Choo, B.S. (1996), "The experimental behaviour of a full-scale semi-rigidly connected composite frame: Detailed appraisal", *J. Const. Steel Res.*, **39**(3), 193-220.

Liew, J.Y.R., Teo, T.H. and Shanmugam, N.E. (2004), "Composite joints subject to reversal of loading-Part 1: Experimental study", *J. Const. Steel Res.*, **60**(5), 221-246.

Liu, J. and Astaneh-Asl, A. (1989), "Cyclic testing of simple connections includeing effect of slab", *J. Struct. Eng.*, **115**(8), 1977-1998.

Plumier, A. and Schleich, J.B. (1993), "Seismic resistance of steel and composite frame structures", *J. Const. Steel Res.*, **27**, 159-176.

Pradhan, A.M. and Bouwkamp, J.G. (1994), "Structural performance aspects on cyclic behaviour of the composite beam-column joints", In *Behaviour of Steel Structures in Seismic Areas STESSA94,* ed. F.M. Mazzolani and V. Gioncu, E&FN SPON, London, 221-230.

Sheikh, T.M., Deierlein, G.G., Yura, J.A. and Jirsa, J.O. (1989), "Beam-column moment connections for composite frames: Part I", *J. Struct. Eng.,* ASCE, **115**(11), 2858-2876.

Simões da Silva, L., Simões, Rui D. and Cruz, Paulo J.S. (2001), "Experimental behaviour of end-plate beam-to-column composite joints under monotonical loading", *Eng. Struct.*, **23**, 1383-1409.

Xiao, Y., Choo, B.S. and Nethercot, D.A. (1994), "Composite connections in steel and concrete - I. Experimental behaviour of composite beam-column connections", *J. Const. Steel Res.*, **31**(1), 3-30.

Yang, Li (2004), "Behaviors study on semi-rigid composite joints under low cyclic loading", M. Eng. Thesis, Nanjing University of Technology.

Zandonini, R., Bernuzzi, C. and Bursi, O. (1997), "Steel and Steel-concrete composite joints subjected to seismic actions", *Proc. of Steel Structures in Seismic Areas* (Kyoto, August, 1997).